

ROLE OF RADIO-FREQUENCY ABLATION IN MANAGEMENT OF LUNG TUMORS

An Essay

*Submitted for the Partial Fulfillment of
The Master Degree in Radio diagnosis*

Presented by

Ahmed Mohammed Abd elmagid Tobar

M .B, B. Ch

Supervised by

Prof. Dr. Mohammed Zaki Elhedk

Professor of Radio diagnosis

Faculty of Medicine

Ain Shams University

Dr. Togan Taha

Lecturer of Radio diagnosis

Faculty of Medicine

Ain Shams University

Faculty of Medicine
Ain Shams University

2012

List of Contents

Title	Page No.
Introduction & Aim of the work.....	1
Lung Anatomy.....	3
Pathology of lung tumors.....	56
Physical Principles.....	80
Technique.....	93
Illustrative Cases.....	131
Summary and Conclusion.....	145
References.....	147
Arabic Summary	

List of Figures

Figure No.	Title	Page No.
Fig. (2-1):	Anatomy of the lung	3
Fig. (2-2):	Anatomical relationship of the extra-thoracic trachea	5
Fig. (2-3):	Anatomical relationship of the main bronchi.....	6
Fig. (2-4):	Illustration of the main, lobar and segmental bronchial division	9
Fig. (2-5):	Topography of the right lung; medial view	11
Fig. (2-6):	Topography of the left lung; medial view	11
Fig. (2-7):	Diagram showing lung lobes and fissures	13
Fig. (2-8):	Bronchopulmonary segments.....	16
Fig. (2-9):	The major divisions of the mediastinum.....	19
Fig. (2-10):	Diagram showing the components of the pleura	21
Fig. (2-11):	Lymphatic drainage of the lungs.....	27
Fig. (2-12):	PA chest radiograph.....	31
Fig. (2-13):	lateral chest radiograph.....	34
Fig. (2-14):	Examination of the seated patient (a) Linear probe placed longitudinally on the right parasternal line. (b) Corresponding sonographic longitudinal panoramic image. K cartilage at the point of insertion of the rib, ICR intercostal space, M muscle, P line of the pleura	36
Fig. (2-15):	Examination of the seated patient. (a) Linear probe placed parallel to the ribs in the third intercostal space. (b) Corresponding sonographic transverse panoramic image .M muscle, P line of the pleura.....	37
Fig. (2-16):	Trans hepatic examination (a) Convex probe placed subcostally from the right. Slight tilting in cranial direction. (b) Corresponding sonographic image. L liver, LV liver vein, ZF diaphragm, S reflection of the liver above the diaphragm.....	38
Fig. (2-17):	Examination from the lateral aspect (a) Convex probe placed longitudinally in the mid portion of the right axillary line. (b) Corresponding sonographic image. D diaphragm. The normal mobile lung is shifted during inspiration into the phrenicocostal recess and covers the upper margin of the liver.....	39
Fig. (2-18):	Chest wall with normal smooth visceral pleura (arrow1).On the outside, the echo-poor pleural gap (arrow 2) and then the echogenic (echo-rich) parietal pleura (arrow 3). The extra pleural fatty lamella varies in strength. The seemingly	

	thicker visceral pleura is actually an artifact due to reflection of the air-containing lung	40
Fig. (2-19):	Clearly recognizable double contour in the area of the parietal pleura (arrow), corresponding with the actual parietal pleura and endothoracic fascia. Note the disproportionately thick visceral pleura (arrowheads) due to artifact	41
Fig. (2-20):	Numerous comet-trail artifacts on the diaphragmatic pleura (white arrow). Given the existing pleural effusion, the comet-trail artifacts are likely due to a partial collapse of the lung and not an expression of an interstitial parenchymal pathology of the lung.....	42
Fig. (2-21):	a)CT lung window. B) CT mediastinal window	47
Fig. (2-22):	a. A-D: Segmental bronchi. (A): Aortic arch (and distal trachea) level. The apical segmental bronchus (arrow) of the right upper lobe is seen. (B): Carinal level. The apical posterior segmental bronchus is demonstrated (solid curved arrow). Anterior segment of the right upper lobe (straight arrow) and posterior segment branch (curved arrow) are also seen. (C): Left pulmonary artery level .The cephalad of the apicoposterior segmental bronchus (straight arrow) and horizontal course of the anterior segment are depicted at this level. (D): Right pulmonary artery level. The bronchus intermedius (small arrow) is seen, with its thin posterior wall .On the left, the bifurcation of the left upper lobe (curved arrow) and lower lobe (straight arrow) are visible.....	51
Fig. (2-23):	a. (Cont..) E-G: (E): Slightly lower level. On the left, the lingular segment (black arrow) is seen. The origin of the middle lobe bronchus is seen on the right (arrowhead). Note the origins of the superior segment bronch bilaterally (white arrows). (F): Left atrial level. The right middle lobe bronchus (black arrow) is seen anterior to the right lower lobe bronchus (white arrow). The left lower lobe bronchus is also demonstrated (white arrow). (G): Segmental bronchi .Curved arrows demonstrate the lateral basal segments bilaterally. Note the posterior basal segment bronchi (straightarrows).....	52
Fig. (2-24):	Vascular anatomy of pulmonary hila. A: Contrast-enhanced computed tomography scan depicting the vascular components of the pulmonary hila. AA, ascending aorta; PA, main pulmonary artery. Arrow: right upper lobe vein. V, left upper lobe pulmonary vein. Arrowhead: superior segment right lower lobe pulmonary artery. B: At a slightly lower level. L, left lower lobe pulmonary artery. arrow: right upper	

lobe pulmonary vein. The right atrial appendage is visible (A). R: right pulmonary artery. C: The superior vena cava is seen sandwiched between the right atrial appendage and the right upper lobe pulmonary vein (white arrow), and the black arrow demonstrates the proximal left coronary artery. V, left upper lobe vein; D: PV, left and right lower lobe pulmonary veins. LAA, left atrial appendage; RA, right atrium.....53

Fig. (3-1): Adenocarcinoma: Peripheral mass located immediately under visceral pleura, with pleural retraction. Tumor has spread along lymphatics, causing widened interlobular septa (Lymphangitis carcinomatosa).....64

Fig. (3-2): Squamous cell carcinoma, note whitish endobronchial obstructive mass.....66

Fig. (3-3): Large cell lung carcinoma in a 64-year-old man. Fused FDG PET/CT images of the chest show extension of the lung mass (white arrow) into the aortopulmonary window; this extension caused paralysis of the left vocal cord due to involvement of the left recurrent laryngeal nerve, thus explaining the asymmetric metabolism of the vocal cords. Also marked narrowing of the left pulmonary artery (black arrows) by the mass, thus illustrating the detail seen with PET/CT. Arrowheads in aortic arch.....67

Fig. (3-4): Small cell carcinoma, large central mass unsheathes bronchi and blood68

Fig. (3-5): Typical carcinoid in a 35-year-old woman with recurrent pneumonia. Chest CT scan (lung window) demonstrates marked cystic bronchiectasis of the left lung. A carcinoid of the left mainstem bronchus was treated with pneumonectomy70

Fig. (4-1): Ionic agitation from alternating current causes tissue coagulation through frictional heating80

Fig. (4-2): Needle of RITA system (Christmas tree needle).....89

Fig. (4-3): Needle of radiotherapeutic system (umbrella needle)91

Fig. (4-4): Single and cluster needle92

Fig. (5-1): CT and gross pathologic appearances of ablated metastasis. (a) Preprocedure planning CT with lung windows shows 14-mm left lower lobe nodule (arrow). (b) Axial image with 3.5-cm electrode array (arrow) deployed eccentrically around lesion (c) Postprocedure CT with lung window shows area of hemorrhage around ablated lesion (white arrow), with small pneumothorax (black arrow), which was asymptomatic and resolved spontaneously. (d) Gross pathology of resected specimen shows ablated lesion (black arrow) eccentrically

	located within ablation zone (outlined by white arrows). No viable cells were seen microscopically.....	104
Fig. (5-2):	Grounding pads properly attached to the patient's thighs, equidistant to the RF site	106
Fig.(5-3):	CT suite during lung RFA. The electrode has been percutaneously introduced into the lung tumor and the position of the deployed tines is monitored in three planes	109
Fig. (5-4):	CT image of the ablated lesion of the patient shown in Fig 36, at mediastinal indow setting. The lesion is totally necrotized immediately after the radiofrequency ablation	111
Fig. (5-5):	CT image obtained 6 months after radiofrequency ablation. The ablated lesion of the patient shown in Fig.36 appears hypo dense, unenhanced and decreased in size. These findings indicate complete ablation	111
Fig. (5-6):	CT image obtained 6 months after radiofrequency ablation. These findings indicate complete ablation.....	112
Fig. (5-7):	Contrast enhanced follow-up CT image at one year reveals local Recurrence of the lesion.....	112
Fig. (5-8):	(A) CT scan showing biopsy-proven left upper lobe metastasis from colon cancer. (B) Radiofrequency ablation of the lesion with adjacent parenchymal hemorrhage and ground glass changes. (C) Follow-up CT scan 1 month post ablation demonstrates an enlarged ablation zone that gradually regresses at the 6-month follow up CT scan (D) and at the 1-year follow-up study (E).....	115
Fig. (5-9):	Persistent symptomatic procedure-related pneumothorax in a 78-year-old woman with a history of heavy cigarette smoking and emphysema and biopsy-proven 2-cm NSCLC in the right upper lobe who refused lobectomy (a) CT scan of lung window demonstrates RF electrode within targeted tumor during RF ablation. In addition to pneumothorax (arrowheads), intraparenchymal hemorrhage (arrow) is noted. (b) Intraprocedurally, an 8-F pigtail catheter was placed to drain the pneumothorax. The patient had a persistent air leak and incomplete reexpansion of the lung with chest tube suction. A large-bore chest tube was placed but the air leak persisted. The patient underwent a conversion to a water seal and discharged home 13 days after RF ablation. Anteroposterior chest radiograph (c) 40 days after RF ablation, immediately before removal of the surgically placed large-bore chest tube, shows that the pneumothorax remained stable; the patient remained asymptomatic.	119

Fig. (5-10):	Fatal pulmonary abscess of bronchocavitary and cavitary-cutaneous fistulas in a 44-year-old woman with stage IIIB NSCLC of the right upper lobe previously treated with chemotherapy and external-beam irradiation. RF ablation was performed for relief of chest and shoulder pain and possible prolongation of life by cytoreduction of the tumor. (a) CT scan of soft-tissue windows with RF electrode located in the deep portion of the tumor. Note the proximity of the electrode tines to the anterior segment of the right upper-lobe bronchus (arrow). Three weeks after RF ablation, the patient experienced progressive dyspnea over several days. CT scans of lung windows (b,c) demonstrate an air-containing necrotic abscess in the region of RF ablation with fistulous connection to the anterior segmental bronchus (arrow) and skin via the previous RF electrode tract (arrowheads). The patient died 7 weeks after RF ablation as a result of progressive respiratory distress and airspace disease despite aggressive antibiotic therapy, attempts to close the bronchial fistula with an endoscopically placed covered stent, and repeated transcavitary catheter-directed administration of biologic adhesive (fibrin glue followed by bovine albumin) and catheter drainage of the abscess cavity.	122
Fig. (5-11):	Cerebral gas microembolization during RF ablation in a 66-year-old man with an isolated 6.6-cm × 4.0-cm right middle-lobe metastasis from squamous-cell carcinoma of the esophagus. The patient had undergone an esophagectomy with colonic pull-through 1 year earlier. (a) CT scan of lung windows with the RF electrode positioned along the deep aspect of the tumor. (b) Duplex US of right internal carotid artery at baseline immediately before RF ablation shows no microembolic Doppler signals. (c) On duplex US image at the same location as b during RF ablation just before roll-off, arrows denote multiple bidirectional discrete “blips” caused by gas microemboli. (d) CT scan of lung windows at the same level as a shows that the necrotic tumor has cavitated with a residual thin wall. Note preservation of the large adjacent pulmonary vessel, presumably as a result of the heat-sink effect.	125
Fig. (6-1):	Case 1	131
Fig. (6-2):	A, CT scan of chest shows recurrent neoplasm (arrow) in radiation field after initial complete response with chemoradiation therapy.	132

Fig. (6-3):	B, CT scan obtained during radiofrequency (RF) ablation shows position of electrode in mass.	133
Fig. (6-4):	C, Supine CT scan obtained immediately after RF ablation and removal of electrode shows increased parenchymal density and peripheral ground-glass opacity around tumor corresponding to lesion induced by RF heat. Note absence of pneumothorax.	133
Fig. (6-5):	D, CT scan obtained at same level as C 6 weeks after C shows mass has become smaller and retracted toward hilum.	134
Fig. (6-6):	Case 3	135
Fig. (6-7):	Case 4	136
Fig. (6-8):	Case 5	137
Fig. (6-9):	Case 6	139
Fig. (6-10):	Case 7	141
Fig. (6-11):	Case 8	143
Fig. (6-12):	Case 9	144

List of Tables

Table No.	Title	Page No.
Table (2-1):	Right lung.....	15
Table (2-2):	Left lung.....	15
Table (2-3):	Lower limits of the lung and pleura.....	20
Table (3-1):	Primary tumor (T) staging.....	73
Table (3-2):	Regional lymph nodes (N) staging	74
Table (3-3):	Distant metastasis (M) staging	75
Table (3-4):	TNM-staging system	76
Table (3-5):	Signs and symptoms of pulmonary carcinoma: Pathologic correlation.....	78
Table (5-1):	Selection Criteria to determine When to Use RFA	101
Table (5-2):	Types of complications	117

LIST OF ABBREVIATIONS

<i>NSCLC</i>	<i>: NON SMALL CELL LUNG CANCER</i>
<i>LMSB</i>	<i>: LEFT MAIN STEM BRONCHUS</i>
<i>RMSB</i>	<i>: RIGHT MAIN STEM BRONCHUS</i>
<i>CT</i>	<i>: COMPUTED TOMOGRAPHY</i>
<i>FDA</i>	<i>: FOOD & DRUG ADMINISTRATION</i>
<i>GGO</i>	<i>: GROUND GLASS OPACIFICATION</i>
<i>HU</i>	<i>: HOUSEFIELD UNIT</i>
<i>mA</i>	<i>: MILLIAMPER</i>
<i>MHZ</i>	<i>: MEGA HERTZ</i>
<i>KHZ</i>	<i>: KILO HERTZ</i>
<i>MRI</i>	<i>: MAGNETIC RESONANCE IMAGING</i>
<i>RF</i>	<i>: RADIOFREQUENCY</i>
<i>RF A</i>	<i>: RADIOFREQUENCY ABLATION</i>
<i>PA</i>	<i>: POSTERO-ANTERIOR</i>
<i>CXR</i>	<i>: CHEST X-RAY</i>
<i>AP</i>	<i>: ANTERO-POSTERIOR</i>
<i>MM</i>	<i>: MILLI METER</i>
<i>CM</i>	<i>: CENTIMETER</i>
<i>IVC</i>	<i>: INFERIOR VENA CAVA</i>
<i>SVC</i>	<i>: SUPERIOR VENA CAVA</i>
<i>TB</i>	<i>: TUBERCULOSIS</i>
<i>DNA</i>	<i>: DEOXYRIBONUCLEIC ACID</i>
<i>BAC</i>	<i>: BRONCHIOLOALVEOLAR CARCINOMA</i>
<i>SCC</i>	<i>: SQUAMOUS CELL CARCINOMA</i>
<i>PET</i>	<i>: POSITRON EMISSION TOMOGRAPHY</i>
<i>LCNEC</i>	<i>: LARGE CELL NEUROENDOCRINE CARCINOMA</i>
<i>SCLC</i>	<i>: SMALL CELL LUNG CARCINOMA</i>
<i>WHO</i>	<i>: WORLD HEALTH ORGANIZATION</i>
<i>UICC</i>	<i>: UNION INTERNATIONALE CONTRE LE CANCER</i>
<i>AJCC</i>	<i>: AMERICAN JOINT COMMITTEE ON CANCER</i>
<i>RML</i>	<i>: RIGHT MIDDLE LOBE</i>
<i>HCC</i>	<i>: HEPATO CELLULAR CARCINOMA</i>
<i>MIN</i>	<i>: MINUTE</i>
<i>W</i>	<i>: WATT</i>
<i>FDG</i>	<i>: FLUORODEOXYGLUCOSE</i>
<i>DWI</i>	<i>: DIFFUSION WEIGHTED IMAGING</i>
<i>GY</i>	<i>: GRAY</i>
<i>CEA</i>	<i>: CARCINOEMBRYONIC ANTIGEN</i>
<i>PT</i>	<i>: PROTHROMBIN TIME</i>
<i>INR</i>	<i>: INTERNATIONAL NORMALIZED RATIO</i>
<i>US</i>	<i>: ULTRASONOGRAPHY</i>



LUNG ANATOMY

1-Gross Lung Anatomy

Overview

The anatomy of the respiratory system can be divided into 2 major parts, airway anatomy and lung anatomy.

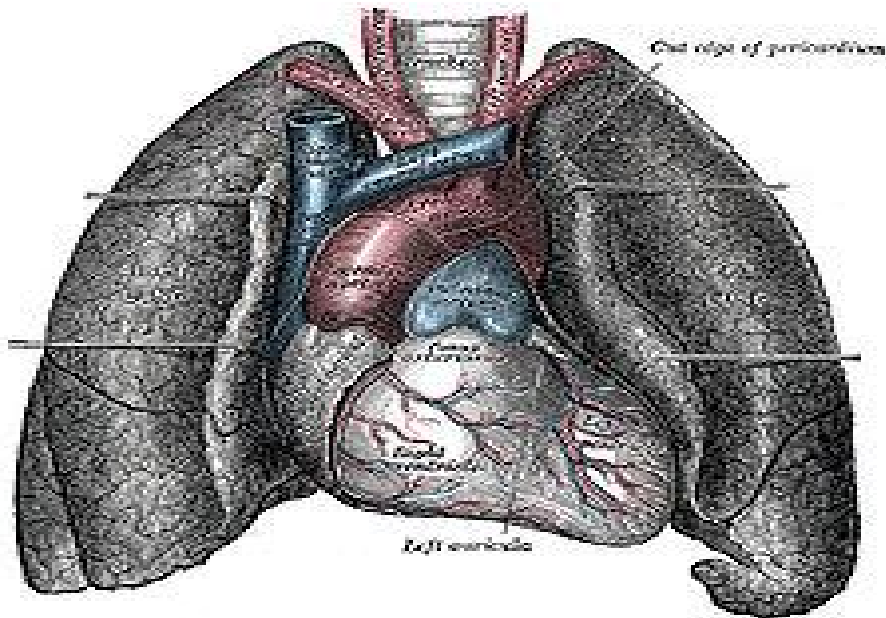


Fig.(2-1): *Anatomy of the lung (Standring, 2005).*

ANATOMY OF THE TRACHEOBRONCHIAL TREE

Trachea

A single tube represents the entrance to the lung's airways between the entrance and periphery lies a meticulously designed system of branching airways that serve to conduct the inspired air into those peripheral channels that carry alveoli in their walls and can thus contribute to the exchange of gases between air and blood (*Fishman's et al., 2008*).

The trachea extends from the larynx, which fixes it through the hyoid bone to the skull, down to its bifurcation in the mediastinum at the level of the fifth thoracic vertebra. Its length varies with movements of the head and respiration but averages about 10–12cm in the adult (*Seaton et al., 2000*).

Anatomical relation:

Its extra-thoracic portion extends down to the sixth cartilage and is closely related to the thyroid gland laterally and its isthmus anteriorly. The recurrent laryngeal nerves also run laterally, beneath the thyroid, while the oesophagus is directly behind, separating it from the vertebrae (*Seaton et al., 2000*).

As it enters the chest, the trachea is related anteriorly to the remains of the thymus, the left innominate vein, the right innominate artery and the left common carotid artery. To its right are the innominate vein, superior vena cava and azygos vein, while on its left

lies the aortic arch. The left recurrent laryngeal nerve runs up between the aortic arch and trachea and then in the ridge between the trachea and oesophagus (*Seaton et al., 2000*).

The trachea is oval in cross-section, being slightly longer in transverse than in sagittal diameter. The tracheal cartilages are semicircular, the gap being in the posterior part where the circle is completed by a 'membranous' portion. The cartilages are connected to each other by fibrous tissue extending from their perichondrium (*Seaton et al., 2000*).

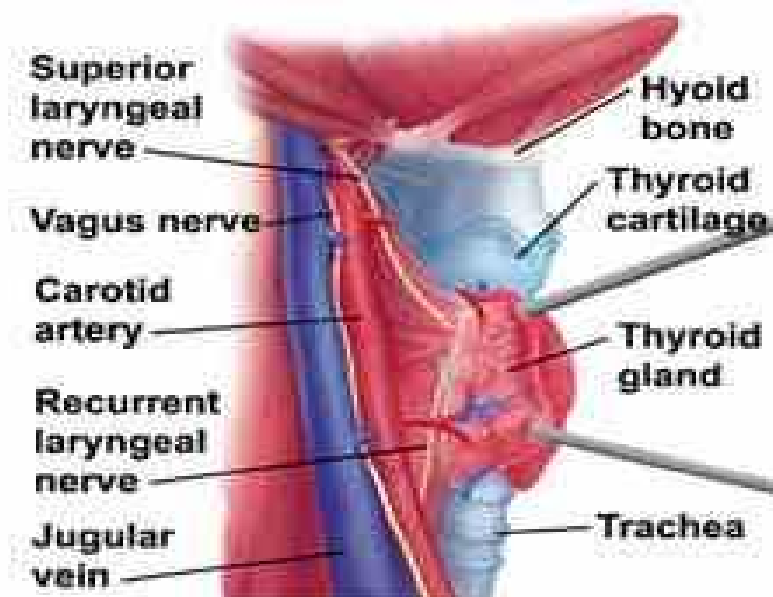


Fig.(2-2): *Anatomical relationship of the extra-thoracic trachea (quoted from yoursurgery.com).*

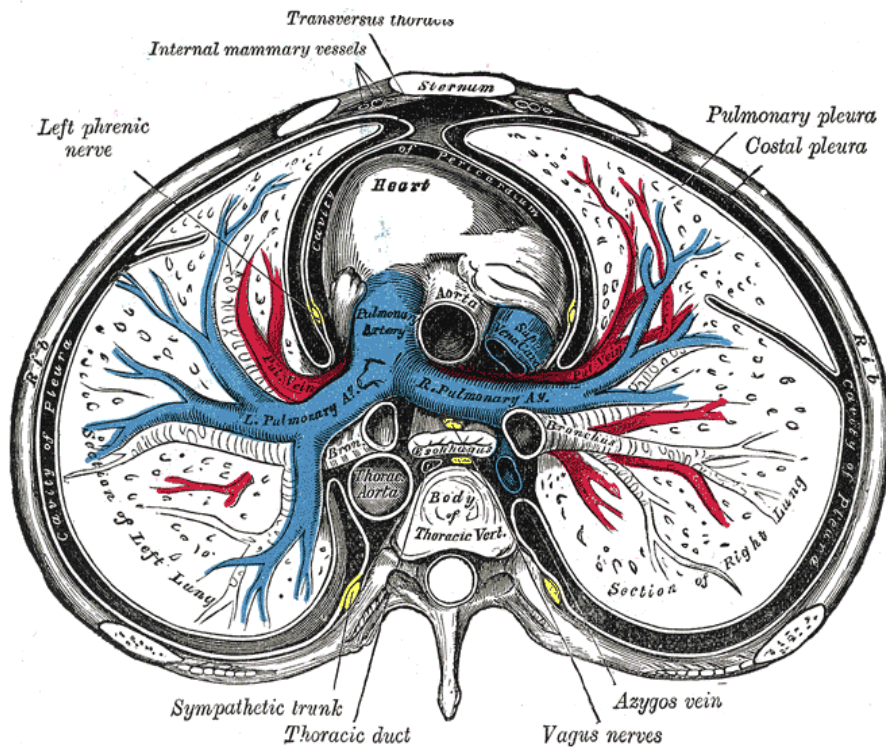


Fig.(2-3): Anatomical relationship of the main bronchi (quoted from Gray's Anatomy, education.yahoo.com)

Bronchi and their divisions:-

The trachea divides into right and left main bronchi at the carina. The carina resides approximately at the level of the fifth thoracic vertebral body (Thompson, 2003).